Biol. Chem., Vol. 390, pp. 1171–1183, November 2009 • Copyright © by Walter de Gruyter • Berlin • New York. DOI 10.1515/BC.2009.127

Plasmodium falciparum glyoxalase II: Theorell-Chance product inhibition patterns, rate-limiting substrate binding via Arg^{257}/Lys^{260}, and unmasking of acid-base catalysis

Miriam Urscher and Marcel Deponte*

Butenandt Institute for Physiological Chemistry, Ludwig Maximilians University, D-81377 Munich, Germany

* Corresponding author
e-mail: marcel.deponte@gmx.de

Abstract

Glyoxalase II (GloII) is a ubiquitous thioester hydrolase catalyzing the last step of the glutathione-dependent conversion of 2-oxoaldehydes to 2-hydroxycarboxylic acids. Here, we present a detailed structure-function analysis of cGloII from the malaria parasite *Plasmodium falciparum*. The activity of the enzyme was salt-sensitive and pH-log k_{cat} and pH-log k_{cat}/K_m profiles revealed acid-base catalysis. An acidic pK_a^{app} value of approximately 6 probably reflects hydroxide formation at the metal center. The glutathione-binding site was analyzed by site-directed mutagenesis. Substitution of residue Arg^{154} caused a 2.5-fold increase of K_m^{app}, whereas replacements of Arg^{257} or Lys^{260} were far more detrimental. Although the glutathione-binding site and the catalytic center are separated, six of six single mutations at the substrate-binding site decreased the k_{cat}^{app} value. Furthermore, product inhibition studies support a Theorell-Chance Bi Bi mechanism with glutathione as the second product. We conclude that the substrate is predominantly bound via ionic interactions with the conserved residues Arg^{257} and Lys^{260}, and that correct substrate binding is a pH- and salt-dependent rate-limiting step for catalysis. The presented mechanistic model is presumably also valid for GloII from many other organisms. Our study could be valuable for drug development strategies and enhances the understanding of the chemistry of binuclear metallohydrolases.

Keywords: binuclear metallohydrolase; catalysis; glutathione; glyoxalase system; hydroxide formation; malaria.

Introduction

Electrophilic 2-oxoaldehydes are harmful chemicals that are formed in every cell and that need to be metabolized because of their ability to modify nucleophiles in proteins and nucleic acids. Methylglyoxal, for example, can be generated as an unwanted byproduct during glycolysis owing to the elimination of phosphate from glyceraldehyde-3-phosphate or dihydroxyacetone-phosphate. Conversion of methylglyoxal and other 2-oxoaldehydes to 2-hydroxycarboxylic acids is catalyzed by the ubiquitous glyoxalase system (Figure 1). The system comprises reduced glutathione (GSH) as a coenzyme as well as the enzymes glyoxalase I and II (GloI, EC 4.4.1.5 and GloII, EC 3.1.2.6). In this pathway, the 2-oxoaldehyde spontaneously reacts with GSH to form two diastereomeric hemithioacetals. These are subsequently isomerized to a thioester by GloI. The thioesterase GloII, which is systematically named *S*-2-hydroxyacylglutathione hydrolase, catalyzes the last step of the pathway leading to the regeneration of GSH and the formation of a 2-hydroxycarboxylic acid (Penninckx et al., 1983; Vander Jagt, 1989; Thornalley, 1990, 1996).

The glyoxalase system is considered to play an important role under pathophysiological conditions (such as, diabetes and renal failure) that are coupled to elevated advanced glycation end products (Penninckx et al., 1983; Nagaraj et al., 1996; Thornalley, 1996; Brinkmann Frye et al., 1998; Oya et al., 1999; Miller et al., 2006). Moreover, GloI and/or GloII have gained attention as a potential drug target in several parasitic protozoa and cancer cells having high glycolytic fluxes that lead to an increased formation of methylglyoxal. These cells require an efficient detoxification system for harmful methylglyoxal and might therefore be highly susceptible to inhibition (Vander Jagt et al., 1990; Hamilton and Creighton, 1992; Elia et al., 1995; Creighton et al., 2003; Tsuruo et al., 2003; Irsch and Krauth-Siegel, 2004; Akoachere et al., 2005; Padmanabhan et al., 2006; Sousa Silva et al., 2008).

The glyoxalase system of the malaria parasite *Plasmodium falciparum* (comprising one functional GloI, one so far inactive GloI-like protein, and two GloII isozymes) has been cloned and basically characterized previously (Iozef et al., 2003; Akoachere et al., 2005). A detailed analysis of the GloI from *P. falciparum* revealed that the monomeric enzyme has two allosterically coupled active sites with different substrate affinities (Deponte et al., 2007). Thus, it might be difficult to completely inactivate the enzyme with a specific inhibitor, and GloII of the parasite might be better suited as a drug target. For example, it has been shown in yeast that the absence of a cytosolic or mitochondrial GloII leads to pronounced growth inhibition upon addition of exogenous methylglyoxal even in the presence of active GloI (Bito et al., 1997). Of the two *P. falciparum* GloII, one isozyme is probably localized in the cytosol (cGloII). The other isozyme carries a putative N-terminal targeting sequence (tGloII) (Akoachere et al., 2005). To date, the precise function of additional GloII isozymes in alternative organelles, such as mitochondria, is unclear (Bito et al., 1997; Cordell et al., 2004; Marasinghe et al., 2005) but other thioesters than *S*-D-lactoylglutathione might be the physiological substrate.

GloII has an N-terminal β-lactamase domain and a C-terminal domain containing five α-helices. Owing to the conserved zinc-binding motif in the β-lactamase fold, the

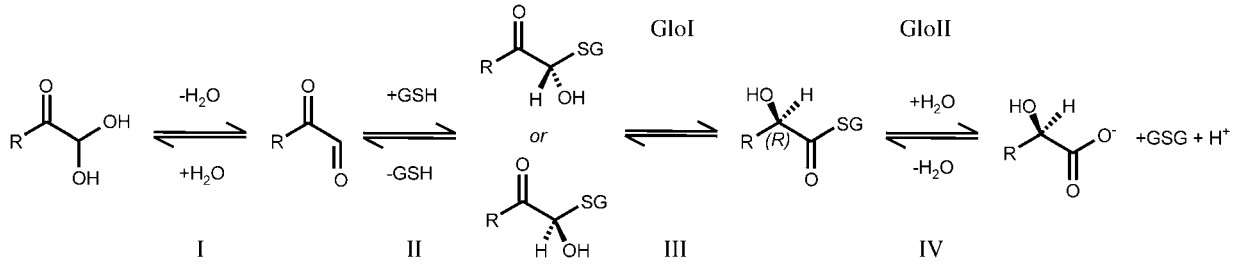

Figure 1 Scheme of the glyoxalase-catalyzed reactions.
The conversion of hydrated 2-oxoaldehydes to 2-hydroxycarboxylic acids occurs in four steps and requires GSH as well as the enzymes GloI and GloII. For example, dehydrated methylglyoxal (R=CH_3) and GSH form two hemithioacetals (step II) that are converted to *S*-D-lactoylglutathione by GloI (step III). The thioester is subsequently hydrolyzed by GloII yielding D-lactate and GSH (step IV).

protein is a member of the structurally diverse group of binuclear metallohydrolases (Cameron et al., 1999; Marasinghe et al., 2005; Campos-Bermudez et al., 2007). The active site can be separated into the catalytic center where hydrolysis takes place and the substrate-binding site. (i) The catalytic center: binuclear metallohydrolases have in common that the two (transition) metal ions at the active site generate a nucleophile (e.g., an activated water molecule or hydroxide ion) and/or are coordinated to an oxygen atom of the substrate. The latter interaction probably stabilizes the transition state and/or polarizes the oxygen bond leading to an increased electrophilicity of the substrate (Mitic et al., 2006). (ii) The substrate-binding site: a co-crystallographic study on human GloII in complex with a glutathione thioester substrate analog previously suggested that the substrate is mainly bound via its glutathione-moiety (Cameron et al., 1999). This could explain why many different *S*-2-hydroxyacylglutathione and even *S*-acylglutathione substrates but no non-glutathione thioesters are efficiently hydrolyzed by the enzyme (Uotila, 1973). Beside two aromatic residues, three basic residues are conserved at the glutathione-binding sites of GloII from man, *Arabidopsis thaliana*, and *Salmonella typhimurium* (Cameron et al., 1999; Marasinghe et al., 2005; Campos-Bermudez et al., 2007). The contribution of these residues to substrate binding has not been studied systematically yet.

Here, we present the characterization of the potential drug target cGloII from *P. falciparum* with an emphasis on structure-function relationships at the active site. Our data support the conclusion that substrate binding (i) is mainly achieved via ionic protein-glutathione interactions and (ii) is a rate-limiting step occurring at a similar rate as product formation. Steady-state kinetics of our and previous studies are in accordance with a Theorell-Chance mechanism. We furthermore suggest that acid-base catalysis is essential for GloII activity and that formation of the hydroxide ion as a nucleophile at the metal center is coupled to a pK_a^{app} value of approximately 6. The results lead to an updated and much more detailed model of the catalytic mechanism of GloII in general.

Results

Sequence alignments and molecular models

A molecular model of the glutathione-binding site of *P. falciparum* cGloII is shown in Figure 2. The distances

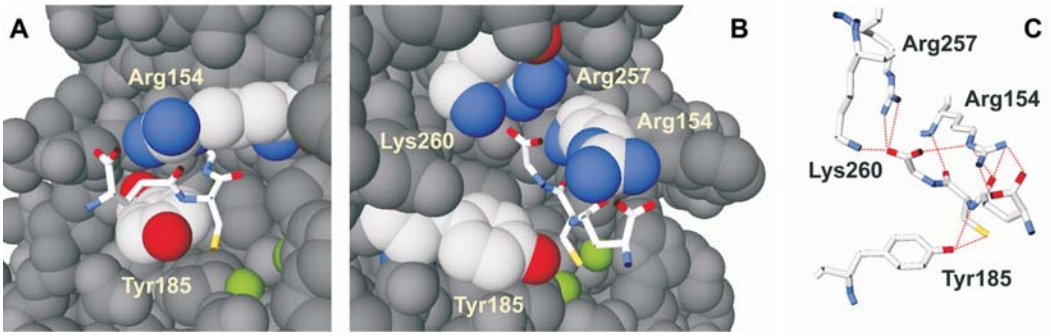

Figure 2 Molecular model of the glutathione-binding site of cGloII.
Residues involved in substrate binding are highlighted. Metal ions at the catalytic center where hydrolysis takes place are shown in green. Glutathione is shown in licorice representation. (A) Side view. (B) Front view. (C) Potential hydrogen bonds between the heteroatoms of cGloII and glutathione are indicated. The distance between the side chain heteroatoms of Arg^{257} and Lys^{260} is $\geq$4.5 Å. The side chain of residue Arg^{154} is approximately 10 Å away from the metal ion center. The distances between the metal ion center and residues Arg^{257} and Lys^{260} are approximately 11 and 13 Å, respectively. These residues are shielded from the reaction center by the glutathione backbone. The model is based on the structure of human GloII (PDB accession number 1QH5) (Cameron et al., 1999). See text for further details.

between the (water-activating) binuclear metal ion center and the basic side chains of residues Arg^{154}, Arg^{257}, and Lys^{260} are $\geq$10 Å. The three residues and the catalytic center are furthermore separated by the glutathione backbone which is sandwiched between residues Arg^{154} and Tyr^{185}. Positively charged ω-nitrogen atoms of Arg^{154} could interact with the α-carboxylate group of the glutamyl-moiety of glutathione. The hydroxyl group of Tyr^{185} points to the cysteinyl sulfur atom and could form hydrogen bonds with the substrate. The α-carboxylate group of the glycine-moiety is bonded to the positively charged ω-nitrogen atoms of Arg^{257}, the ε-nitrogen atom of Lys^{260}, and the δ-nitrogen atom of Arg^{154}. The latter bond is absent in many other GloII because of a lysine substitution (e.g., in the human enzyme and in tGloII). All other glutathione interactions, including Tyr^{185} and the two positively charged amino acids close to the C-terminus, are highly conserved among GloII from different organisms (alignments not shown). This is also the case for tGloII having insertions before helix α7 and the C-terminal helix α8 that were incorrectly aligned in a previous study (Akoachere et al., 2005). Thus, most of the conclusions described below probably also apply to many other glyoxalases, except for the trypanothione-dependent GloII from kinetoplastids having a significantly altered substrate-binding site (Irsch and Krauth-Siegel, 2004; Padmanabhan et al., 2006; Sousa Silva et al., 2008).

Generation and purification of wild type cGloII and glutathione-binding site mutants

To study the influence of Arg^{154}, Arg^{257}, and Lys^{260} on catalysis, two single mutants were generated for each residue by site-directed mutagenesis. Recombinant N-terminally MRGS(H)$_6$GS-tagged cGloII wild type and mutant enzymes were all soluble and of high purity as determined by SDS-PAGE (Figure 3A). Depending on the mutant, the average yield was between 25 and 70 nmol (0.8–2.2 mg) of protein per liter of *Escherichia coli* culture. Correct folding of wild type and mutant enzymes was confirmed by circular dichroism (CD) spectroscopy (Figure 3B) and gel filtration chromatography (data not shown). The purified enzymes became inactivated during storage as reported for human GloII (Uotila, 1973): wild type cGloII lost between 20% and 50% of its initial activity after 5 d storage, and the mutants lost between 30%

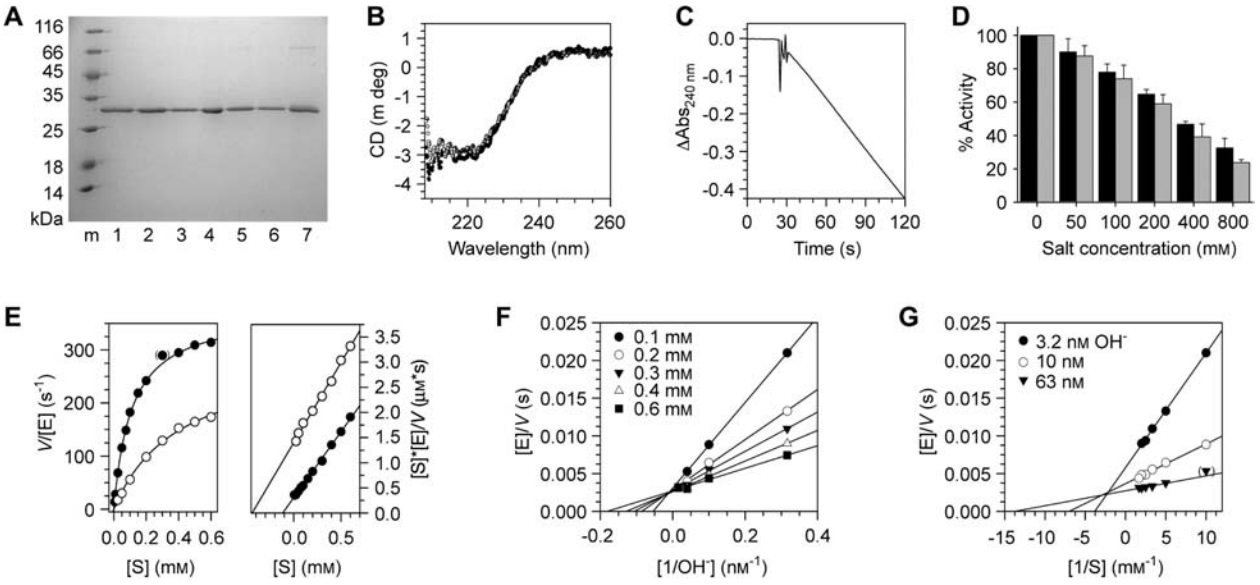

Figure 3 Purified cGloII has a salt- and pH-sensitive activity and complies with Michaelis-Menten kinetics.
(A) Recombinant enzymes were purified by Ni-NTA chromatography and the purity was confirmed by reducing SDS-PAGE. A summary of representative eluates of wild type and mutant enzymes is shown on a 15% gel. The calculated molecular mass of His-tagged cGloII is 31.8 kDa. Lanes: m, marker; 1, wild type cGloII; 2, cGloII^{R154K}; 3, cGloII^{R154M}; 4, cGloII^{R257D}; 5, cGloII^{R257Q}; 6, cGloII^{K260D}; 7, cGloII^{K260Q}. (B) CD spectra of 12 μM cGloII^{K260D} and wild type enzyme (open and closed circles, respectively). Although cGloII^{K260D} had a much lower catalytic efficiency (Table 1), the spectrum was very similar to the wild type enzyme. The secondary structure content (26% α-helices and 26% β-strands) could only be estimated owing to the strong absorbance of the buffer at wavelengths $\leq$210 nm. (C) Enzymatic activity with *S*-D-lactoylglutathione as a substrate was monitored at 25°C. A representative time course of a single measurement with 5 nM wild type enzyme and 0.4 mM substrate is shown. A baseline was recorded for 30 s before the assay was started by the addition of enzyme. Very similar results were obtained when the assay was started with substrate. (D) Activity of wild type enzyme significantly decreased with increasing salt concentration in the assay mixture. Measurements with 0.4 mM substrate were performed with KCl (black bars) and NaCl (gray bars). (E) Enzymatic activity followed Michaelis-Menten kinetics. Data from a representative experiment with wild type enzyme are shown in a direct plot (left) and a Hanes plot (right). Values for K_m^{app} and k_{cat}^{app} in the absence of additional salt (closed circles) were 111±3 μM and 374±3 s^{-1}, respectively. When 0.4 mM NaCl was present in the assay mixture (open circles), the K_m^{app} value increased to 402±30 μM and the k_{cat}^{app} value decreased to 297±12 s^{-1}. (F) Enzymatic activity was also monitored at pH 5.5–6.8 using the indicated concentrations of *S*-D-lactoylglutathione. Data from a single experiment with wild type enzyme are shown in a Lineweaver-Burk plot yielding a rather constant k_{cat}^{app} value. (G) The *S*-D-lactoylglutathione-dependency of enzymatic activity at the indicated OH^- concentrations yielded a rather constant intersection point in the Lineweaver-Burk plot at -3 mM^{-1}.

and 50% of their activity after 2 d. Thus, all steady-state kinetic assays for the determination of K_m^{app} and k_{cat}^{app} values were performed directly after purification yielding reproducible results.

Metal content analysis, and salt and pH dependencies

A previous metal analysis of cGloII was not conclusive and showed a rather low metal content of 0.05 mol of zinc and 0.26 mol of iron per mol of protein (Akoachere et al., 2005). We therefore optimized the expression/purification protocol and re-evaluated the metal content of the enzyme. Under the chosen conditions, recombinant wild type and all mutant enzymes were saturated with $\geq$2 mol of zinc per mol of protein. No manganese, copper, molybdenum, or cobalt and only small traces of iron ($\sim$0.1 mol) were found in the protein eluates.

The improved protocol was also reflected by a 3-fold increase of $k_{cat}^{app}=V/[E]_0$ for the wild type enzyme with *S*-D-lactoylglutathione as a substrate (Table 1). The determined K_m^{app} value of 0.1 mM confirmed previous results on recombinant enzyme (Akoachere et al., 2005) and parasite extracts (Vander Jagt et al., 1990). The catalytic efficiency of cGloII was similar to enzymes from man (Ridderström et al., 1996), *A. thaliana* (Ridderström and Mannervik, 1997), and yeast (Bito et al., 1999) but was approximately 20-fold lower than for *A. thaliana* Glx2-2 (Zang et al., 2001) (Table 1). Activity of wild type cGloII (Figure 3C,E) and the mutant enzymes (data not shown) followed typical Michaelis-Menten kinetics in the substrate concentration range tested. A salt concentration-activity profile revealed that the enzyme was far less active when salt was present in the assay. The activity with 0.4 mM substrate dropped below 50% at salt concentrations above 0.4 M (Figure 3D). Moreover, the catalytic efficiency at 0.4 M NaCl was reduced to less than one-fourth of the catalytic efficiency in the absence of salt due to an increased K_m^{app} value and a decreased k_{cat}^{app} value (Figure 3E). Loss of activity was not coupled to protein precipitation and a salt-sensitive enzymatic activity is in agreement with experiments on human GloII (Uotila, 1973). All other kinetic measurements were therefore performed with salt-free assay buffers and the final salt concentration was kept below 5 mM even when high enzyme concentrations (e.g., for cGloII^{R257D}) were required. The enzymatic activity of cGloII was also highly pH-dependent, which is not surprising considering (i) the acidic and basic groups of the substrate and the active site and (ii) the potential involvement of a hydroxide ion as the nucleophile: varying the *S*-D-lactoylglutathione concentration between 0.1 and 0.6 mM and the pH from 5.5 to 6.8 (corresponding to a hydroxide concentration between 3 and 63 nM), and plotting the reciprocal reaction velocity versus the reciprocal concentration of the hydroxide ion in the assay, yielded straight lines. The common intersection point of these lines was above the *x*-axis and close to or almost at the *y*-axis (Figure 3F). Plotting the reciprocal reaction velocity versus the reciprocal *S*-D-lactoylglutathione concentration yielded straight lines with a common intersection point above the *x*-axis and left of the *y*-axis (Figure 3G). The theoretical K_m^{app} value for OH^- determined from the *x*-axis of Figure 3F decreased with an increasing *S*-D-lactoylglutathione concentration and ranged from 20 to 6 nM under the chosen assay conditions. The K_m^{app} value for *S*-D-lactoylglutathione determined from the *x*-axis of Figure 3G also decreased with an increasing hydroxide ion concentra-

Table 1 Steady-state kinetic parameters of wild type and mutant GloII from different organisms.

Enzyme	k_{cat}^{app} (s^{-1})[a]		K_m^{app} (μM)[a]		k_{cat}/K_m (M^{-1} s^{-1})[a]	
cGloII WT[b]	120	(32%)	100±10	(88%)	1.2×10^6	(36%)
cGloII WT	375±61	(100%)	114±12	(100%)	3.3×10^6	(100%)
cGloII^{R154K}	285±65	(76%)	116±14	(102%)	2.4×10^6	(73%)
cGloII^{R154M}	222±48	(59%)	275±34	(241%)	8.1×10^5	(25%)
cGloII^{R257Q}	67±32	(18%)	[i]2551±130	(2238%)	3.0×10^4	(0.9%)
cGloII^{R257D}	60±30	(16%)	[i]5782±3074	(5072%)	1.1×10^4	(0.3%)
cGloII^{K260Q}	171±37	(46%)	[i]4308±1200	(3779%)	4.1×10^4	(1.2%)
cGloII^{K260D}	74±43	(20%)	[i]2867±1409	(2515%)	2.6×10^4	(0.8%)
A. thaliana Glx2-2 WT[c]	3930±138	(100%)	63±10	(100%)	6.2×10^7	(100%)
A. thaliana Glx2-2^{K144A} [c,d]	1760±170	(45%)	170±53	(270%)	1.0×10^7	(16%)
A. thaliana Glx2-2^{R250W} [e,d]	484±92	(12%)	600±100	(952%)	8.1×10^5	(0.8%)
Human GloII WT[f,g]	780	(100%)	187	(100%)	4.2×10^6	(100%)
Yeast Glo2 WT[h,g]	979	(100%)	112	(100%)	8.7×10^6	(100%)
Yeast Glo4 WT[h,g]	723	(100%)	72	(100%)	1.0×10^7	(100%)

[a]All parameters were determined with *S*-D-lactoylglutathione as substrate. Values for cGloII were averaged from at least three independent transformation/expression/purification experiments and are plotted in Figure 5.
[b]Akoachere et al. (2005).
[c]Zang et al. (2001).
[d]Residues Arg^{250} and Lys^{144} of Glx2-2 (GenBank accession number O24496) were described as Arg^{248} and Lys^{142}, respectively.
[e]Crowder et al. (1997).
[f]Ridderström et al. (1996).
[g]The kinetics were analyzed at 37°C in contrast to the other studies that were performed at 25°C.
[h]Bito et al. (1999).
[i]The highest substrate concentration in the assay was 0.7 mM and therefore the accuracy of the higher K_m^{app} values is affected.

tion and ranged from approximately 260 to 75 μM. Although the pH can certainly influence cGloII catalysis in numerous ways, the data suggest a Bi Bi mechanism with the direct involvement of a hydroxide ion as a second substrate (see also below). In summary, recombinant cGloII is zinc-dependent and has a salt- and pH-sensitive activity with Michaelis-Menten kinetics.

Product inhibition studies

Apart from two product inhibition studies on GloII from man and *A. thaliana* yielding different results (Uotila, 1973; Zang et al., 2001), not very much is known about the product release during GloII catalysis. We therefore performed *S*-D-lactoylglutathione hydrolase inhibition studies with wild type enzyme using D-lactate, GSH, or an ethyl ester of glutathione (GSH-EE) as inhibitors. In the latter compound, the carboxylate group of the glycine-moiety (Figure 2) is modified. Reaction kinetics with millimolar concentrations of D-lactate revealed a competitive inhibition pattern as indicated by the parallel lines in the Hanes plot (Figure 4A) and a constant intercept on the *y*-axis in the Lineweaver-Burk plots (Figure 4B). Noncompetitive inhibition profiles were obtained for GSH and GSH-EE (Figure 4A,B). (Please note that we use the term noncompetitive inhibition according to the canonical terminology by Cleland. This type of inhibition is also sometimes referred to as mixed inhibition.) Based on the Lineweaver-Burk plots, we generated secondary plots to determine two different inhibition constants (K_i^{slope} and K_i^{int}). The K_i^{slope} value for D-lactate was 31 nM (Figure 4C) and an identical value was determined from the common intersection point in Dixon plots (Figure 4D). This value usually reflects inhibitor binding to the free enzyme. The lines in Figure 4B intersect above the *x*-axis and as a consequence K_i^{slope} values for GSH and GSH-EE (around 3.5 and 14 mM, respectively) were smaller than the K_i^{int} values (of 13 and 49 mM, respectively) (Figure 4C,D). Thus, substrate binding to the free and occupied enzyme interfered with inhibitor binding and vice versa. Both K_i values for GSH-EE were approximately 3.5-fold higher than for GSH, and accordingly GSH is a stronger inhibitor than GSH-EE.

Residues Arg^{257} and Lys^{260} are more important for substrate binding than Arg^{154}

Mutation of residues Arg^{154}, Arg^{257}, or Lys^{260} had a negative influence on catalysis as summarized in Figure 5. Residue Arg^{154}, which is situated just after a β-hairpin, was replaced with lysine and methionine (as mentioned, lysine is a natural replacement in several other GloII). In contrast to a previous study on an alanine mutant of *A. thaliana* Glx2-2 (Zang et al., 2001), methionine was chosen because of its longer side chain that discriminates more clearly between the structural sandwich function and the charge of Arg^{154} (Figure 2). The K_m^{app} value of cGloII^{R154K} was unchanged (Table 1, Figure 5C), suggesting that the interaction between the δ-nitrogen atom of Arg^{154} and the substrate (Figure 2C) is rather weak. However, as expected, the cationic side chain of the residue was relevant for substrate binding as reflected by a 2.5-fold increase of the K_m^{app} value for cGloII^{R154M}.

A more crucial area for substrate binding is formed by the cationic side chains of residues Arg^{257} and Lys^{260} (Figure 2) as already indicated by the comparative inhibition studies with GSH and GSH-EE (Figure 4). Both basic residues, which are situated at the same side of the C-terminal helix α8, were replaced with aspartate or glutamine because of (i) the similar conformational parameters (Chou and Fasman, 1978), (ii) the ability to form hydrogen bonds, and (iii) the different charges. The estimated K_m^{app} values of all four single mutants were approximately 20- to 50-fold increased (Table 1) pointing to strongly impaired substrate binding properties. A double mutant of both residues (cGloII$^{R257Q/K260Q}$) was inactive at enzyme concentrations up to 0.5 μM (data not shown). The increase of K_m^{app} was more pronounced for cGloII^{R257D} than for cGloII^{R257Q} (Figure 5C), suggesting that not only hydrogen bonds but especially ionic protein-substrate interactions are required for tight substrate binding. (cGloII^{K260Q} and cGloII^{K260D} are difficult to compare, see below.) Strong ionic protein-substrate interactions are also in agreement with the salt-dependent activity of cGloII (Figure 3D,E), because charged protein and substrate side chains become more shielded at higher salt concentrations resulting in a significant decrease of the reaction velocity.

In summary, our kinetic data strongly support the structure-based hypothesis that GSH is predominantly bound through ionic interactions between the α-carboxylate group of the glycine-moiety of the substrate and the side chains of residues Arg^{257} and Lys^{260}. Residue Arg^{154} is also involved in substrate binding but seems to be less important.

Mutations at the substrate-binding site also influence k_{cat} and alter complex pH profiles

Despite the structural separation of the reaction center and the glutathione-binding site (Figure 2), all six of six single mutations had a negative influence on k_{cat}^{app} (Table 1, Figure 5B). Mutants with significantly increased K_m^{app} values also tended to have the lowest k_{cat}^{app} values. Moreover, pH-activity profiles of all mutant enzymes were altered when compared to wild type enzyme (Figure 6A). A striking effect was observed for cGloII^{K260D}, having a highly simplified bell-shaped pH-activity profile with a maximum at pH 6.7 in contrast to the broad asymmetric profiles of the other enzymes. To explain the specific effect observed for cGloII^{K260D}, we re-examined our molecular model and checked for structural changes because of the mutation that could not be seen in the CD spectra. Formation of a novel internal salt bridge between residues Asp^{260} and Arg^{257} was found to be the most probable cause because it neutralizes the basic area at the C-terminal α-helix (Figure 6B). A comparable salt bridge was not found for cGloII^{R257D} which is in accordance with the pH profile.

Comparison of pH-k_{cat} and pH-k_{cat}/K_m profiles of wild type enzyme and cGloII^{K260D} revealed two major ionization states. The data were fitted according to a bell-shaped curve yielding an estimation of two apparent pK_a values (Figure 6C). Similar values were obtained from the logarithmic profiles (Figure 6D). The wild type enzyme and cGloII^{K260D} both had an acidic pK_a^{app} value of ~6 and

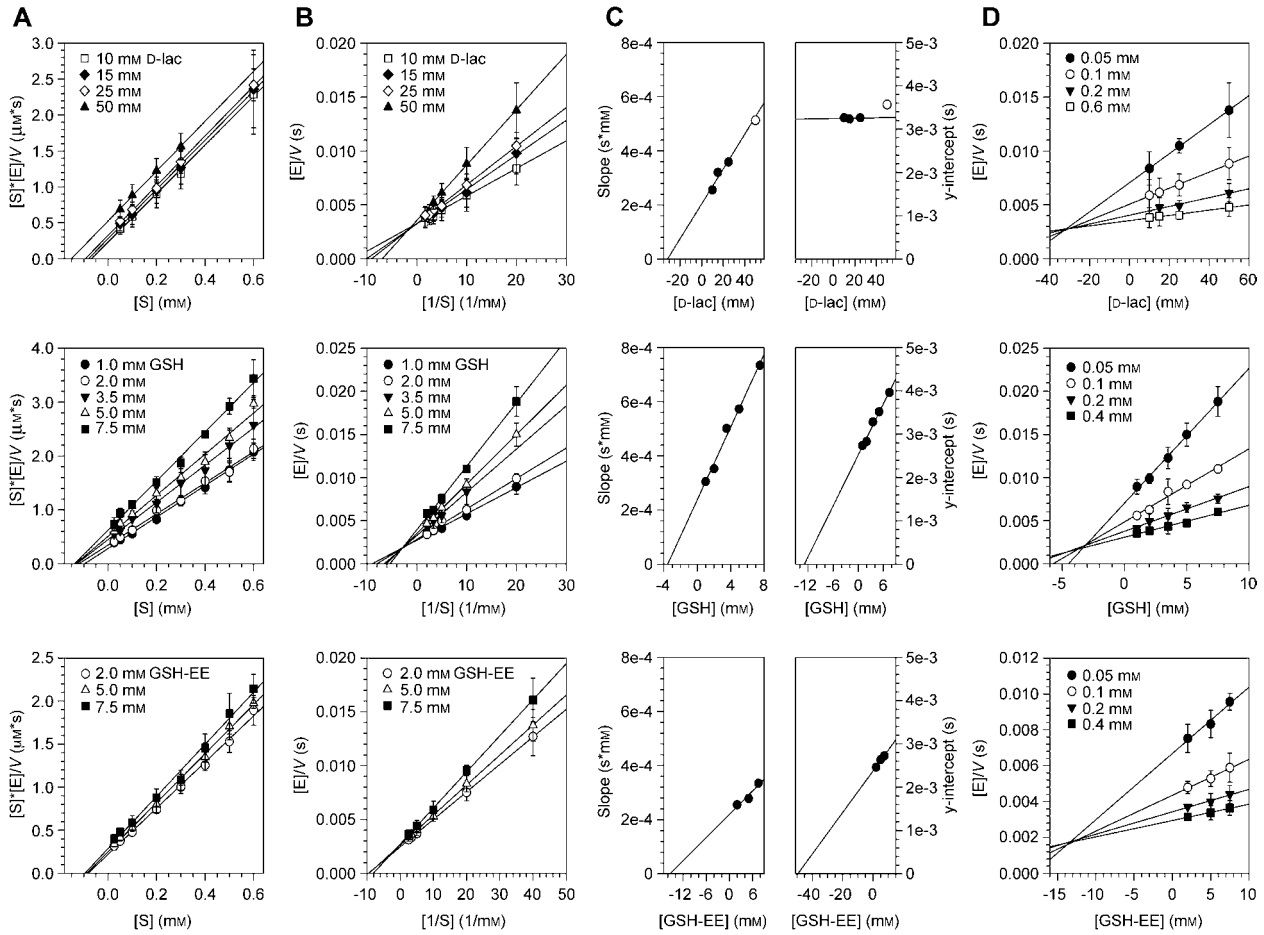

Figure 4 Substrate inhibition studies with D-lactate, GSH, and GSH-EE.
All assays were performed with wild type enzyme at 25°C. The influence of the indicated concentrations of D-lactate (upper row), GSH (middle), and GSH-EE (lower row) on catalysis is shown. Plots according to (A) Hanes and (B) Lineweaver-Burk theory revealed a competitive inhibition pattern for D-lactate and a noncompetitive pattern for GSH and GSH-EE. Secondary plots of the slopes and *y*-intercepts from panel (B) are plotted in (C). $-K_i^{slope}$ and $-K_i^{int}$ values were determined from the *x*-intercept of the secondary plots. At 50 mM lactate, a slight reduction of k_{cat}^{app} was probably due to the salt concentration (open circle). (D) To facilitate comparison with previous studies, inhibition kinetics were also plotted according to Dixon. Values in panels (A)–(D) were averaged from at least three independent experiments.

a basic pK_a^{app} value of ~8.5 in the k_{cat} plots. In the k_{cat}/K_m plots, the pK_a^{app} value of ~6 was only slightly increased, whereas the basic pK_a value was decreased to ~7.5. Even though it was possible to assign two pK_a^{app} values to all curves, it is obvious that the data points did not perfectly fit the simple model. We therefore suggest that there are more than two relevant ionization states. Furthermore, although the pK_a^{app} values of wild type enzyme and cGloII^{K260D} are comparable, the altered shapes of the curves in Figure 6C and D suggest that the mutation of one of the basic residues at the substrate-binding site significantly affected a kinetically relevant pK_a value.

As we will illustrate below, the kinetic parameters as well as the pH profiles and the product inhibition patterns support the conclusion that substrate binding is a rate-limiting step occurring at a similar rate as product formation. The complexity of the pH profiles at higher pH values is probably influenced by the different protonation states of the basic substrate-binding residues, whereas the pK_a^{app} value of approximately 6 could reflect nucleophile formation at the reaction center.

Discussion

The product inhibition patterns are typical for a Theorell-Chance Bi Bi mechanism

GSH and D-lactate inhibition patterns from our studies (Figure 4) are similar to *A. thaliana* Glx2-2 (Zang et al., 2001) but the K_i values of cGloII for GSH and lactate are almost 10-fold increased and decreased, respectively. The K_i values for GSH are much higher than the K_m value. Considering millimolar concentrations of GSH in the cell, this might be a prerequisite for the enzyme to function properly. Zang et al. (2001) suggested (based on inhibition patterns of ordered Uni Bi reactions as described in Segel, 1993) that D-lactate is the first product and GSH is the second product. However, inhibition patterns for such a Uni Bi reaction should be noncompetitive for D-lactate and competitive for GSH, not vice versa (pp. 544–555 in Segel, 1993). Thus, either the mechanistic assumptions are incorrect or GSH is the first product released. The latter possibility cannot be fully excluded but seems rather unlikely considering (i) the K_i values that

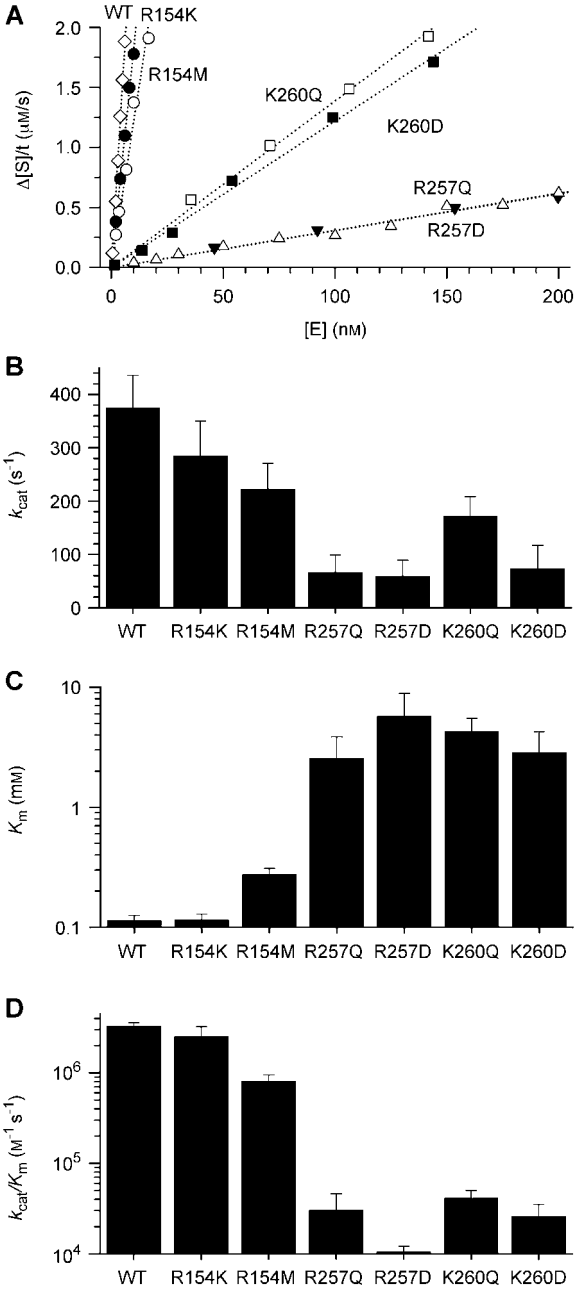

Figure 5 Steady-state kinetic parameters of cGloII.
(A) Enzyme concentration-activity profiles of wild type and mutant enzymes were analyzed with 0.4 mM substrate at 25°C. All enzyme concentrations used for the determination of k_{cat}^{app}, K_m^{app}, and the catalytic efficiency shown in Table 1 and panels (B)–(D) were in the linear concentration range. Values in panels (B)–(D) were averaged from at least three independent transformation/expression/purification experiments.

point to stronger GSH than lactate binding (Figure 4 C,D) (Zang et al., 2001) and (ii) the rather low specificity of glyoxalases for the carboxylic acid-moiety of the substrate (Uotila, 1973). Because catalysis potentially requires hydroxide ions instead of water, the reaction could indeed have two substrates (OH^- and the thioester) and two products. This theory is supported by the data shown in Figure 3F and G. The inhibition patterns with D-lactate and GSH (Figure 4) exclude a ping-pong mechanism, a classical ordered and an iso-ordered Bi Bi mechanism. Instead, the patterns are typical for a Theorell-Chance mechanism (Table II in Rudolph, 1979; pp. 593–606 in Segel, 1993; Table 2.3 in Bisswanger, 2000). Such a rather unusual mechanism was described, e.g., for aminoglycoside phosphotransferase type III converting kanamycin A (McKay and Wright, 1995). The Theorell-Chance mechanism (Scheme 1l0) is a special case of an ordered Bi Bi mechanism in which the concentrations of the enzyme-substrate and the enzyme-product complexes (EAB and EPQ) are essentially close to zero.

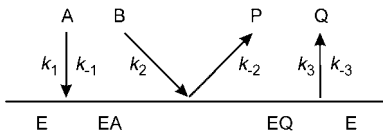

Scheme 1 The Theorell-Chance mechanism.

In other words, the central complexes break down as rapidly as they form. The first product (P) is immediately released, whereas the second product (Q) dissociates more slowly. Following this mechanistic model, cGloII is not fully saturated with the hydroxide ion as first substrate at pH 6.8. This assumption is supported by the theoretical K_m^{app} value for OH^- (Figure 3F) and the pK_a^{app} value of ~6 (Figure 6C,D) as described below. Accordingly, when the concentration of the second substrate *S*-D-lactoylglutathione was varied, inhibition patterns with D-lactate and GSH as the first and the second product had to be competitive and noncompetitive, respectively. The K_i^{slope} and K_i^{int} values can then be interpreted as described in Figures IX-23 and IX-25 in Segel (1993). For example, K_i^{slope} for D-lactate is $K_{ip}=k_3/k_{-2}=31$ mM (Scheme 1). A Theorell-Chance mechanism is also in perfect agreement with our other observations suggesting that the central complex between cGloII, the hydroxide ion, and *S*-D-lactoylglutathione is so instable that both, *S*-D-lactoylglutathione binding and turnover occur at a similar rate. In the following sections, we will first discuss the substrate-binding site and then the reaction center of cGloII with regard to catalysis.

Ionic interactions between the glycine carboxylate group and Arg[257] and Lys[260] control substrate binding

To our knowledge, the only other exhaustive mutational study on the glutathione-binding site of a GloII was on Glx2-2 from *A. thaliana*: Zang et al. (2001) reported that residue Arg^{250} near the C-terminus of the protein was accidentally mutated to tryptophan in a previous study by Crowder et al. (1997). The mutation resulted in a ~10-fold increase of K_m^{app} and a ~12-fold decrease of k_{cat}^{app}. Owing to the introduction of the bulky tryptophan residue in Glx2-2, significant structural changes could not be excluded. Because our mutations in $cGloII^{R257Q}$ and $cGloII^{R257D}$ show a comparable effect on k_{cat}^{app} and K_m^{app} (Table 1), the importance of this residue is now verified. In addition to Arg^{257}, residue Lys^{260} is highly relevant for optimal substrate binding because mutations have a similar drastic effect on K_m^{app} (Figure 5C). A central role of ionic interactions between the substrate glycine carboxylate group and the two basic residues at the substrate-binding site is substantiated by (i) the complex pH

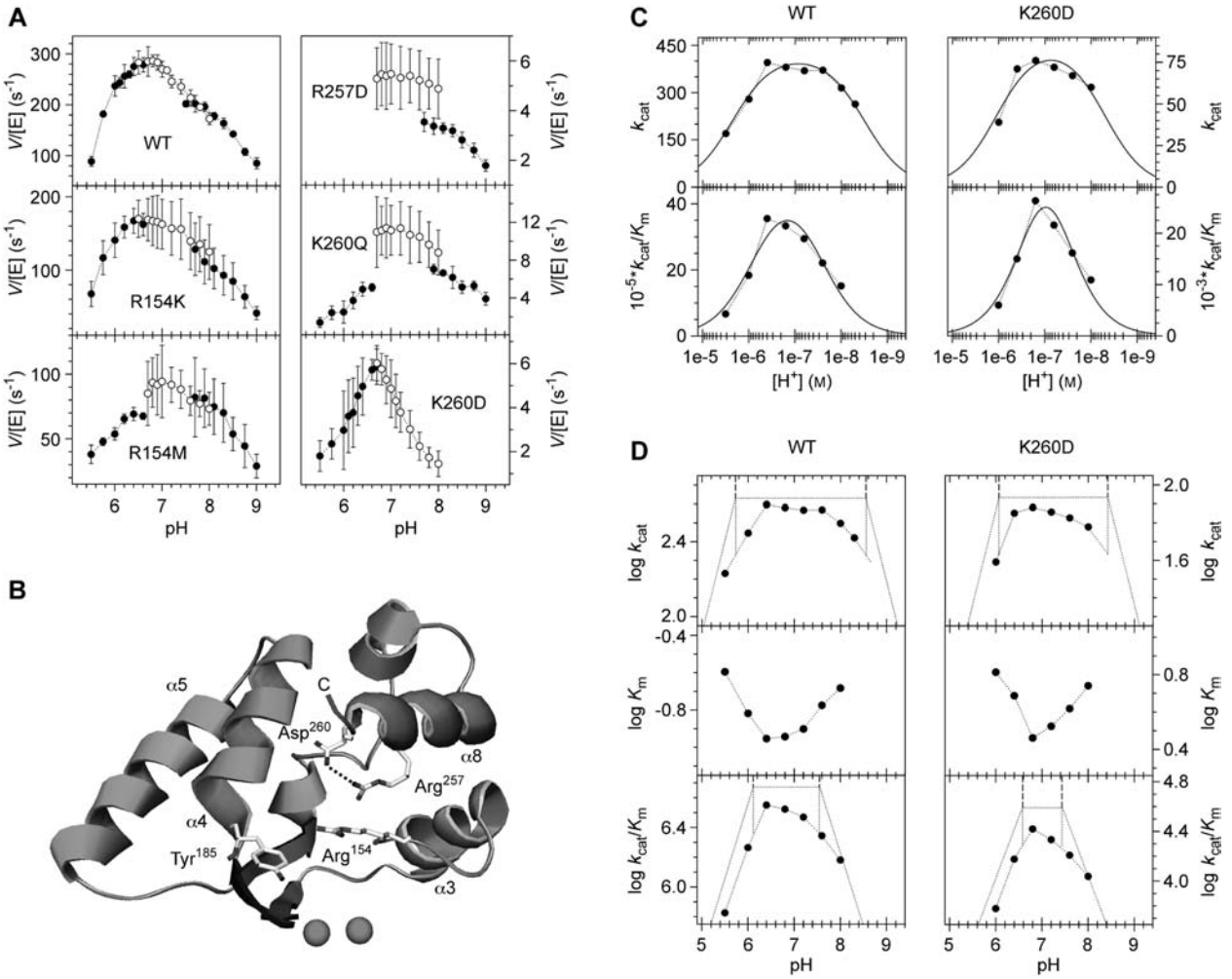

Figure 6 pH profiles of cGloII wild type and mutant enzymes.
(A) All pH-activity profiles were determined with 0.4 mM substrate at 25°C (K_m^{app} values of the proteins are given in Table 1). Data points are the mean of three or more experiments. Three different buffers containing either 100 mM MES (pH 5.5–6.7), 100 mM MOPS (pH 6.5–8.0), or 100 mM Tris (pH 7.5–9.0) were used. (B) A salt bridge could be formed between residues Arg^{257} and Asp^{260} at the C-terminal α-helix in $cGloII^{K260D}$. The side chain of Arg^{257} has the same conformation as in Figure 2. The N-terminal domain has been removed for clarity. (C) pH-k_{cat} and pH-k_{cat}/K_m profiles for wild type enzyme (left) and $cGloII^{K260D}$ (right). Data were fitted using equations $k_{cat}=k_{cat}'/(1+[H^+]/K_1+K_2/[H^+])$ (upper diagrams) and $k_{cat}/K_m=(k_{cat}'/K_m')/(1+[H^+]/K_3+K_4/[H^+])$ (lower diagrams) (Brocklehurst, 1996). The following values for the parameters were estimated by nonlinear regression analysis using SigmaPlot 10.0. Wild type cGloII: $k_{cat}'=420(\pm17)$ s^{-1}; $K_1=2.3(\pm0.5)\times10^{-6}$ M (pH 5.6); $K_2=3.2(\pm0.7)\times10^{-9}$ M (pH 8.5); $k_{cat}'/K_m'=4.9(\pm0.9)\times10^6$ $M^{-1}s^{-1}$; $K_3=7.3(\pm3.3)\times10^{-7}$ M (pH 6.1); $K_4=2.9(\pm1.3)\times10^{-8}$ M (pH 7.5). $cGloII^{K260D}$: $k_{cat}'=86(\pm9)$ s^{-1}; $K_1=1.1(\pm0.5)\times10^{-6}$ M (pH 6.0); $K_2=5.1(\pm2.7)\times10^{-9}$ M (pH 8.3); $k_{cat}'/K_m'=4.1(\pm2.1)\times10^4$ M^{-1} s^{-1}; $K_3=1.9(\pm1.3)\times10^{-7}$ M (pH 6.7); $K_4=4.8(\pm3.4)\times10^{-8}$ M (pH 7.3). (D) pH-log k_{cat}, K_m, k_{cat}/K_m profiles for wild type enzyme (left) and $cGloII^{K260D}$ (right). Straight lines of slope zero were drawn at log k_{cat}' and log k_{cat}'/K_m' using the values from panel (C). Straight lines of slope +1 and -1 were constructed to intersect the lines of slope zero such that the intersection points are above/below the experimental data at the pH of the intersection point by 0.3 (log2) (Brocklehurst, 1996). Estimated pK_a^{app} values are indicated at the *x*-axis for each plot and are in good agreement with values for K_{1-4} determined in panel (C).

profiles at alkaline conditions (Figure 6), (ii) the influence of the salt-concentration on the kinetic parameters (Figure 3D,E), and (iii) the fact that GSH-EE is a weaker inhibitor than GSH (Figure 4).

Mutation of Lys^{144} of *A. thaliana* Glx2-2 to alanine resulted in a moderate ~2.5-fold increase of K_m^{app} and a ~2-fold decrease of k_{cat}^{app} (Zang et al., 2001). The effect was very similar to that of $cGloII^{R154M}$ (Table 1) but the slightly higher impact for the alanine mutation might support the hypothesis that not only the charge but also the longer side chain of the residue is required to clamp the substrate in a correct orientation (Figure 2). Tyr^{185} also plays a role in substrate binding because mutation to phenylalanine led to a 2.5- and 8-fold increase of K_m^{app} in *P. falciparum* cGloII and human GloII, respectively (Ridderström et al., 2000; Akoachere et al., 2005). In summary, mutational analyses of the glutathione-binding site show that the substrate is mainly bound via ionic interactions with residues Arg^{257} and Lys^{260}.

Substrate binding is a rate-limiting step for GloII catalysis

A plausible explanation for the decreased k_{cat}^{app} values of our mutants is that substrate binding and hydrolysis occur at a similar rate. Thus, substrate binding becomes a rate-limiting step. Our theory is in agreement with the Theorell-Chance inhibition patterns and the effect of the mutations on the pH profiles (see below). One might argue that the mutations altered the transition state

geometry of the substrate consequently affecting the rate of hydrolysis and the k_{cat}^{app} value. Indeed, such a scenario could hold true for mutations of residue Tyr^{185} (Figure 2). However, an altered transition state geometry seems to be rather unlikely for the basic residues: even if the glutathione carboxylate groups are significantly rotated or tilted because of the mutated binding site, the thioester bond could still adopt an identical position during catalysis. Furthermore, Arg^{154} is much closer to the reaction center than residues Lys^{260} and Arg^{257} (Figure 2) but the effect on k_{cat}^{app} was much weaker in $cGloII^{R154M}$ than in $cGloII^{R257Q}$ and $cGloII^{K260Q}$ (Figure 6B). The interpretation that the protein-substrate interaction is a rate-limiting step is also in good agreement with previous studies: only small solvent isotope effects were observed for *A. thaliana* Glx2-2 and human GloII (Zang et al., 2001) suggesting that acid-base catalysis (see below) is not the only rate-limiting step. Moreover, the k_{cat}/K_m value of rat GloII decreased markedly with increasing viscosity of the assay buffer using *S*-D-lactoylglutathione as a substrate. When the slow substrate *S*-acetylglutathione was used instead, the influence of the viscosity on k_{cat}/K_m almost disappeared (Guha et al., 1988), and hydrolysis became the predominant rate-limiting step.

Influence of the substrate-binding site on the basic pK_a^{app} values

A macroscopic pK_a value of approximately 9 was previously detected for rat and human GloII (Ball and Vander Jagt, 1981; Allen et al., 1993) and a similar value of ~8.5 could be estimated from our pH-k_{cat} and pH-log k_{cat} plots (Figure 6C,D). Ball and Vander Jagt proposed that the basic pK_a^{app} value can be assigned to the protein and not to the glutathione-moiety. Following their argumentation, we suggest that the two conserved residues Arg^{257} and Lys^{260} at helix α8 both contribute to the basic pK_a^{app}. Apart from the molecular model (Figure 2), four observations support this conclusion: (i) in $cGloII^{K260D}$ the influence of both basic residues was probably reduced (Figure 6B), resulting in a much simpler bell-shaped pH-activity profile (Figure 6A). (ii) The asymmetric distribution of the data points in Figure 6C,D suggests that more than one basic ionization state influenced the kinetics. (iii) Accordingly, mutation of Lys^{260} to aspartate changed the pH-k_{cat} and pH-k_{cat}/K_m profiles (although it did not lead to a simple bell-shaped or even sigmoidal curve in these plots). (iv) The basic pK_a^{app} values determined from pH-log k_{cat} and pH-log k_{cat}/K_m profiles differ significantly for both wild type enzyme and $cGloII^{K260D}$ (Figure 6C,D). Because pK_a^{app} values from pH-log k_{cat}/K_m and pH-log k_{cat} plots can be often assigned to the enzyme and the enzyme-substrate complex, respectively (Brocklehurst, 1996), we suggest that the pK_a values of residues Arg^{154}, Arg^{257}, and Lys^{260} are altered upon interaction with the substrate. In addition, the pH profiles and the basic pK_a^{app} value could be influenced by acid-base catalysis at the binuclear metal center (see below).

cGloII mutants have unaltered metal binding sites and are correctly folded

Metal binding seems to be variable in GloII. Studies on human enzyme revealed ~1.5 mol of zinc and 0.7 mol of iron per mol of protein (Cameron et al., 1999), and a 1:1 ratio of zinc to iron was found for GloII from *Trypanosoma brucei* (Irsch and Krauth-Siegel, 2004). Glx2-2 and Glx2-5 from *A. thaliana* and GloB from *S. typhimurium* bind either two zinc ions, a Fe(III)Zn(II) center, a Fe(III)Fe(II) center, or even a Mn(II)Mn(II) center (Zang et al., 2001; Schilling et al., 2003; Marasinghe et al., 2005; Campos-Bermudez et al., 2007). Our data revealed that all recombinant cGloII constructs were saturated with zinc and were correctly folded (Figure 3B). Thus, the reduced activities of the mutant enzymes (Figure 5) were not caused by insufficient saturation of the metal-binding site or protein misfolding. A zinc-dependent activity is in agreement with studies on *P. falciparum* tGloII (Akoachere et al., 2005), and GloII from *A. thaliana* (Crowder et al., 1997) and *E. coli* (O'Young et al., 2007) which were also shown to contain two zinc ions per protein molecule. The different metal compositions of recombinant glyoxalases could depend on the growth conditions, might be coupled to second sphere ligands, and do not seem to have a drastic influence on the catalytic efficiency (Schilling et al., 2003; Marasinghe et al., 2005; Campos-Bermudez et al., 2007). The latter observation becomes explainable considering substrate binding once again as a rate-limiting step.

GloII acid-base catalysis

The zinc ions of the binuclear metallohydrolase cGloII are thought to bind, activate or generate the nucleophile at the reaction center. Interpreting the pK_a^{app} values from pH-log k_{cat}/K_m and pH-log k_{cat} plots as the pK_a^{app} values of the enzyme and the enzyme-substrate complex, respectively, free cGloII and the enzyme-thioester complex both have a comparable acidic pK_a^{app} value of ~6 (Figure 6D). We suggest that this value reflects formation of the hydroxide ion at the metal center. Indeed, a pK_a value <7 is not unusual for the water ligand of a binuclear metallohydrolase and is also found, e.g., in purple acid phosphatases (Mitic et al., 2006). Based on previous inactivation studies using diethyl pyrocarbonate (Ball and Vander Jagt, 1981), we speculate that one of the histidine residues at the reaction center could be the proton acceptor. The acid-base catalyst could subsequently transfer the proton to the thiolate leaving group (and such a step could influence the basic pK_a^{app} value). Unmasking of acid-base catalysis and of the hydrolytic step with a pH optimum of 6.7 is a plausible explanation for the bell-shaped pH-activity profile of $cGloII^{K260D}$ (Figure 6A): at a pH below the acidic pK_a^{app} value of ~6, the local concentration of the highly nucleophilic hydroxide ion decreased significantly resulting in the lowered activity of wild type enzyme and $cGloII^{K260D}$ (Figure 6C,D). At a pH above the pK_a^{app} value of ~7.5, a proton transfer between an active site residue and the substrate might have been impaired. A similar pK_a^{app} value was also detected for free wild type enzyme in the k_{cat}/K_m plots (Figure 6C,D). In the pH-activity profiles and the k_{cat} plots of wild type enzyme, the value could be shifted because of the kinetic relevance of the basic substrate binding residues (see above). In summary, our studies point to nucleophile formation at pH 6 and provide experimental evidence for acid-base catalysis being usually masked in GloII because of the rate-limiting substrate binding step.

Summary of the reaction mechanism

A refined model of the catalytic mechanism of GloII is shown in Figure 7. The scheme is based on enzyme kinetic data from this work, as well as on crystallographic studies (Cameron et al., 1999; Marasinghe et al., 2005; Campos-Bermudez et al., 2007) and general considerations on the catalytic mechanism of binuclear metallohydrolases (Mitic et al., 2006). Upon substrate binding, the carboxylate group of the glutathione glycine-moiety is anchored via ionic interactions with residues Arg^{257} and Lys^{260} (step I in Figure 7). Residues Arg^{154} and Tyr^{185} are required for weaker interactions and form a clamp leading to a correct orientation of the substrate. Reaction I is one of the rate-limiting steps for cGloII catalysis. Once the substrate is bound, the immediate nucleophilic attack of the hydroxide ion results in a tetrahedral transition state that could be thermodynamically favored due to the interaction with the metal center (step II). After hydrolysis, the liberated carboxylic acid could shortly interact with the first metal ion, whereas the thiolate leaving group could be stabilized by the second cation before it is protonated (step III). Owing to the different free energies of species b and d (Creighton et al., 1988), the equilibrium of the hydrolysis lies on the side of the products. According to a Theorell-Chance mechanism, D-lactate is rapidly released (step IV). GSH is more tightly bound and is therefore the second product which is probably released more slowly (step V). The next water molecule could enter the accessible active site right after the release of D-lactate. Interaction of the coordinated water molecule with the binuclear metal center drastically lowers the pK_a resulting in efficient hydroxide formation at physiological pH (step VI). The acidic pK_a^{app} value for hydroxide formation is quite similar in species F and B. In contrast, the basic pK_a^{app} value differs between both species and could reflect the relevance of the residues at the metal center and the glutathione-binding site.

Impact on drug development strategies

It is controversial whether the glyoxalase system can be exploited for drug development and this might highly depend on the investigated organism and cell type. On the one hand, computer simulations suggested that the glyoxalases from different organisms might be a poor drug target (Sousa Silva et al., 2005). Indeed the knockout of a trypanothione-dependent GloII from *Trypanosoma brucei* did not result in severe growth defects for procyclic (insect) parasite stages, and knockdown experiments with bloodstream forms were also discouraging (Wendler et al., 2009). On the other hand, a recent

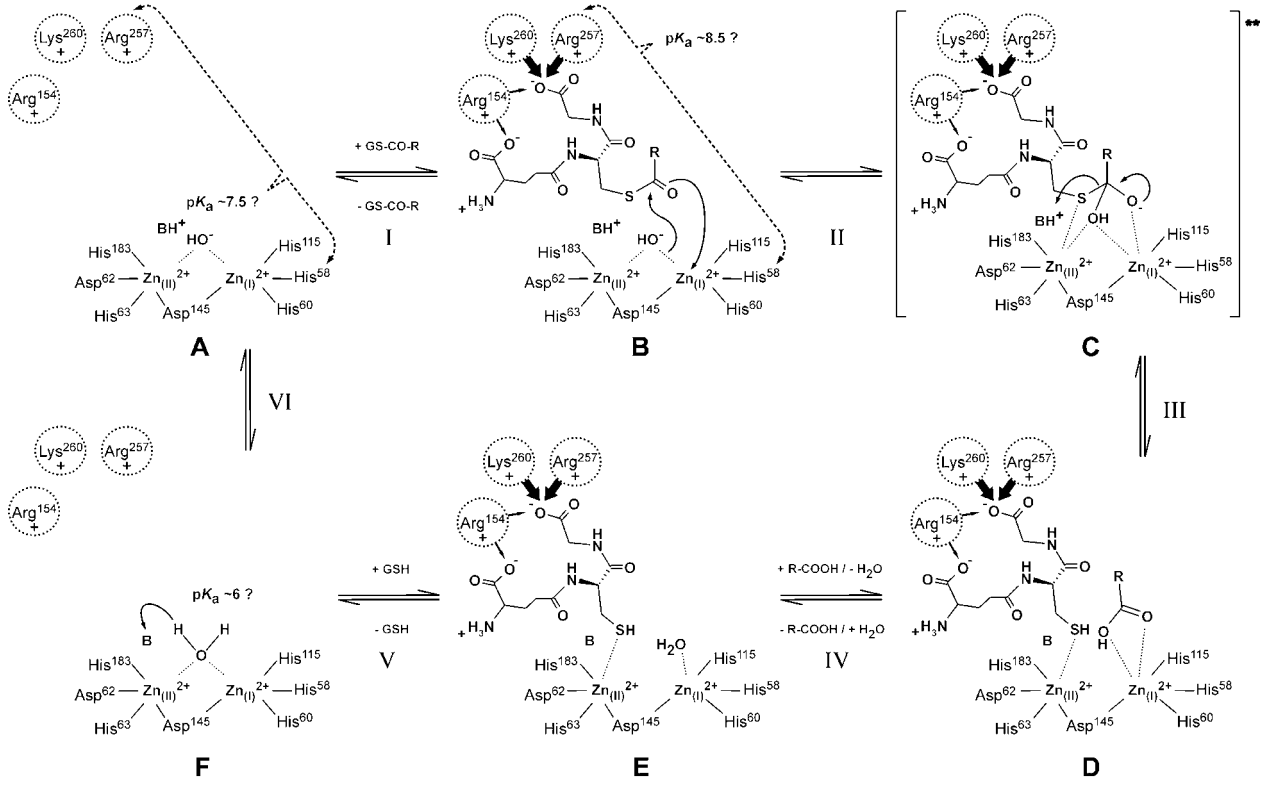

Figure 7 Proposed mechanism of thioester hydrolysis by cGloII.
The thioester substrate is mainly bound via the conserved basic residues. Weak and strong electrostatic protein-substrate interactions are indicated by thin and thick arrows, respectively. The nucleophile is generated at the binuclear metal center. The first zinc ion ($Zn_{(I)}^{2+}$) is coordinated by His^{58} Nε2, His^{60} Nδ1, and His^{115} Nε2. The second zinc ion ($Zn_{(II)}^{2+}$) is coordinated by Asp^{62} Oδ2, His^{63} Nε2, and His^{183} Nε2. Residue Asp^{145} bridges both ions but is closer to $Zn_{(II)}^{2+}$. One of the histidine residues presumably serves as an acid-base catalyst (*B*). Putative interactions between the substrates and the metal ions during catalysis are indicated by dotted lines. Hydroxide ion formation could have a pK_a^{app} value of approximately 6. The second pK_a^{app} value of free enzyme and the thioester complex (Figure 6C,D) could be affected to a different degree by (i) the protonated substrate-binding residues and (ii) a proton donor at the reaction center. See text for further details.

exhaustive study by Kawatani et al. (2008) identified GloI as the major target of methyl-gerfelin induced inhibition of osteoclastogenesis in cell culture. The essentiality and suitability of *P. falciparum* GloI, cGloII, and tGloII as a drug target remain to be tested. It has been previously shown for human GloII that potent glutathione-based inhibitors can be specific for the enzyme without significant impairment of other glutathione-dependent proteins (Elia et al., 1995). Because some potent inhibitors of GloI are slowly turned over by GloII (e.g., Hamilton and Creighton, 1992), a combination of GloI and GloII inhibitors could result in a high degree of synergism. Considering cGloII as a potential drug target, blocking residues Arg^{257} and/or Lys^{260} could lead to highly efficient inhibition. Depending on the size of the inhibitor, this could also be true for blocking Arg^{154}. The advantages of the latter approach might be (i) that the inhibitor does not compete with a very tightly bound part of the substrate and (ii) that Arg^{154} is replaced by a lysine residue in human GloII resulting in a higher specificity for cGloII.

Materials and methods

Site-directed mutagenesis and heterologous expression of *cGLOII*

cGLOII was cloned into pQE30 (Qiagen, Hilden, Germany) as described previously (Akoachere et al., 2005). Mutations of *cGLOII* were introduced by PCR with *Pfu* polymerase (Promega, Mannheim, Germany) using mutated primers and the wild type *cGLOII*/pQE30 construct as a template. Methylated non-mutated template plasmids were digested with *Dpn*I (NEB, Frankfurt, Germany), and competent XL1-Blue cells or EZ cells (Qiagen) were subsequently transformed. Correct sequences of all mutants were confirmed by DNA sequencing both strands. *cGLOII* constructs were expressed in *E. coli* strain XL1-Blue. Bacteria were precultured overnight at 37°C in Luria-Bertani (LB) medium supplemented with 100 mg/l ampicillin. The preculture was diluted (between 1:25 and 1:50) and grown at 37°C to an optical density at 600 nm of 0.3. Then, 286 mg/l $ZnSO_4 \cdot 7H_2O$ was dissolved in the medium and the culture was grown for a further 30 min before induction with 0.5 mM isopropyl-β-D-1-thiogalactopyranoside. Cells were harvested 4 h after induction by centrifugation (15 min, 4000 *g*, 4°C), washed once with buffer containing 300 mM NaCl, 50 mM 3-(N-morpholino)propanesulfonic acid (MOPS)/NaOH, pH 7.8, and stored at -20°C.

Protein purification and analysis

Bacteria were thawed on ice and resuspended in 7.5 ml buffer containing 300 mM NaCl, 10 mM imidazole, 50 mM MOPS/NaOH, pH 7.8 per liter of culture. After addition of lysozyme and DNaseI, the suspension was stirred for 1 h on ice, followed by sonication at 4°C and centrifugation (30 min, 30 500 *g*, 4°C). The supernatant was applied to a Ni-NTA column (Qiagen), which was equilibrated with the same buffer. The column was washed with eight column volumes of 300 mM NaCl, 25 mM imidazole, 50 mM MOPS/NaOH, pH 7.8, and recombinant enzyme was eluted with 4.5 column volumes of 300 mM NaCl, 125 mM imidazole, 50 mM MOPS/NaOH, pH 7.8. Protein concentrations of the fractions were determined using the Bradford assay with bovine serum albumin as standard (Bradford, 1976), and the sample purity was confirmed by reducing sodium dodecyl sulfate-polyacrylamide gel electrophoresis (SDS-PAGE) (Laemmli, 1970). The metal content of freshly purified cGloII was analyzed in a central facility of the Ludwig-Maximilians University by inductively coupled plasma atomic emission spectroscopy (ICP-AES) using a Varian Vista RL CCD simultaneous ICP-AES spectrometer and the software ICP expert (Varian, Darmstadt, Germany). Elution buffer without protein served as negative control. The secondary structure and the content of folded protein were analyzed by CD spectroscopy at the Max Planck Institute of Biochemistry using a Jasco J-810 spectropolarimeter (Jasco, Groß-Umstadt, Germany). Before analysis, the protein samples were repeatedly washed with 300 mM NaCl, 50 mM MOPS/NaOH, pH 7.8 and concentrated in an Amicon Ultra-15 device (Millipore, Schwalbach, Germany) to remove the imidazole. After a clearing spin (15 min, 17 500 *g*, 4°C), the protein concentration was adjusted and spectra were recorded at 4°C. Complete removal of the buffer was impossible due to protein precipitation in pure water. For the estimation of the secondary structure content, a reference spectrum of the buffer was subtracted.

Steady-state kinetics

Steady-state kinetics were monitored spectrophotometrically at 25°C using a thermostatted Jasco V-550 UV-visual spectrophotometer. GloII activity was determined by measuring the thioester hydrolysis of *S*-D-lactoylglutathione (Sigma, Munich, Germany) at 240 nm with an extinction coefficient of 3.1 mM^{-1} cm^{-1} as described previously (Akoachere et al., 2005). Assays for the determination of k_{cat}^{app} and K_m^{app} values were performed in 100 mM MOPS/NaOH, pH 6.8 with the exception of $cGloII^{R257Q}$, which was analyzed at the pH optimum of 7.4. The concentration of *S*-D-lactoylglutathione varied from 5 µM to 0.7 mM. All reactions were initiated by the addition of enzyme. Depending on the enzymatic activity, different final protein concentrations were used for wild type and mutant enzymes in the assay (5–7 nM wild type cGloII, 10 nM $cGloII^{R154K}$ and $cGloII^{R154M}$, 100 nM $cGloII^{K260Q}$ and $cGloII^{K260D}$, 140–180 nM $cGloII^{R257Q}$, and 215–230 nM $cGloII^{R257D}$). Kinetic data of the initial reaction velocities were plotted according to Michaelis-Menten, Lineweaver-Burk, Eadie-Hofstee, and Hanes and fitted using the program SigmaPlot 10.0 (Systat Software, Inc., Erkrath, Germany).

Salt and pH dependencies

The salt dependency of the enzymatic activity was analyzed analogously with wild type cGloII and 0.4 mM *S*-D-lactoylglutathione in assay buffer containing 0–0.8 M NaCl or KCl and 100 mM MOPS/NaOH, pH 6.8. In addition, K_m^{app} and k_{cat}^{app} values were determined as described above with 0.4 M NaCl, 100 mM MOPS/NaOH, pH 6.8 replacing the standard assay buffer. The pH dependency of the enzymatic activity was determined for wild type and mutant enzymes at pH values ranging from 5.5 to 9.0. Three different buffers containing either 100 mM 2-(N-morpholino)ethanesulfonic acid (MES) (pH 5.5–6.7), 100 mM MOPS (pH 6.5–8.0), or 100 mM Tris (pH 7.5–9.0) were used.

Product inhibition studies

GSH, GSH-EE, and D-lactic acid were obtained from Sigma. For the product inhibition studies with wild type cGloII, stock solutions of GSH (100 mM), GSH-EE (250 mM) and D-lactate (1 M) were prepared in assay buffer. The pH was adjusted with NaOH resulting in an unaltered pH of 6.8 in the assays. Substrate and inhibitor were premixed in the cuvette and the assay was started by adding 2 nM wild type cGloII at 25°C.

Sequence alignment and molecular modeling

Sequences of GloII homologs that were identified by BLAST searches were aligned using the program ClustalW (Thompson

et al., 1994). A model of cGloII in complex with GSH was generated based on the structure of complexed human GloII (PDB accession number 1QH5) (Cameron et al., 1999) as described previously (Akoachere et al., 2005).

Acknowledgments

We thank Helmut Hartl for atomic emission spectroscopy, Elisabeth Weyher for her help with CD spectroscopy, and Prof. Katja Becker and Prof. Walter Neupert for their support. We are especially grateful to Keith Brocklehurst for help with the generation and interpretation of pH profiles. This work was supported by the Deutsche Forschungsgemeinschaft grant De1431/1-1.

References

Akoachere, M., Iozef, R., Rahlfs, S., Deponte, M., Mannervik, B., Creighton, D.J., Schirmer, H., and Becker, K. (2005). Characterization of the glyoxalases of the malarial parasite *Plasmodium falciparum* and comparison with their human counterparts. Biol. Chem. *386*, 41–52.

Allen, R.E., Lo, T.W., and Thornalley, P.J. (1993). Inhibitors of glyoxalase I: design, synthesis, inhibitory characteristics and biological evaluation. Eur. J. Biochem. *213*, 1261–1267.

Ball, J.C. and Vander Jagt, D.L. (1981). *S*-2-hydroxyacylglutathione hydrolase (glyoxalase II): active-site mapping of a nonserine thiolesterase. Biochemistry *20*, 899–905.

Bisswanger, H. (2000). Enzymkinetik, 3. Auflage (Weinheim, Germany: Wiley-VCH).

Bito, A., Haider, M., Hadler, I., and Breitenbach, M. (1997). Identification and phenotypic analysis of two glyoxalase II encoding genes from *Saccharomyces cerevisiae*, GLO2 and GLO4, and intracellular localization of the corresponding proteins. J. Biol. Chem. *272*, 21509–21519.

Bito, A., Haider, M., Briza, P., Strasser, P., and Breitenbach, M. (1999). Heterologous expression, purification, and kinetic comparison of the cytoplasmic and mitochondrial glyoxalase II enzymes, Glo2p and Glo4p, from *Saccharomyces cerevisiae*. Protein Expr. Purif. *17*, 456–464.

Bradford, M.M. (1976). A rapid and sensitive method for the quantitation of microgram quantities of protein utilizing the principle of protein-dye binding. Anal. Biochem. *72*, 248–254.

Brinkmann Frye, E., Degenhardt, T.P., Thorpe, S.R., and Baynes, J.W. (1998). Role of the Maillard reaction in aging of tissue proteins. Advanced glycation end product-dependent increase in imidazolium cross-links in human lens proteins. J. Biol. Chem. *273*, 18714–18719.

Brocklehurst, K. (1996). Physical factors affecting enzyme activity. In: Enzymology Labfax, P.C. Engel, ed. (San Diego, CA/Oxford: Academic Press/Bios Scientific Publishers Ltd.), pp. 175–198.

Cameron, A.D., Ridderström, M., Olin, B., and Mannervik, B. (1999). Crystal structure of human glyoxalase II and its complex with a glutathione thiolester substrate analogue. Structure *7*, 1067–1078.

Campos-Bermudez, V.A., Leite, N.R., Krog, R., Costa-Filho, A.J., Soncini, F.C., Oliva, G., and Vila, A.J. (2007). Biochemical and structural characterization of *Salmonella typhimurium* glyoxalase II: new insights into metal ion selectivity. Biochemistry *46*, 11069–11079.

Chou, P.Y. and Fasman, G.D. (1978). Empirical predictions of protein conformation. Annu. Rev. Biochem. *47*, 251–276.

Cordell, P.A., Futers, T.S., Grant, P.J., and Pease, R.J. (2004). The human hydroxyacylglutathione hydrolase (HAGH) gene encodes both cytosolic and mitochondrial forms of glyoxalase II. J. Biol. Chem. *279*, 28653–28661.

Creighton, D.J., Migliorini, M., Pourmotabbed, T., and Guha, M.K. (1988). Optimization of efficiency in the glyoxalase pathway. Biochemistry *27*, 7376–7384.

Creighton, D.J., Zheng, Z.B., Holewinski, R., Hamilton, D.S., and Eiseman, J.L. (2003). Glyoxalase I inhibitors in cancer chemotherapy. Biochem. Soc. Trans. *31*, 1378–1382.

Crowder, M.W., Maiti, M.K., Banovic, L., and Makaroff, C.A. (1997). Glyoxalase II from *A. thaliana* requires Zn(II) for catalytic activity. FEBS Lett. *418*, 351–354.

Deponte, M., Sturm, N., Mittler, S., Harner, M., Mack, H., and Becker, K. (2007). Allosteric coupling of two different functional active sites in monomeric *Plasmodium falciparum* glyoxalase I. J. Biol. Chem. *282*, 28419–28430.

Elia, A.C., Chyan, M.K., Principato, G.B., Giovannini, E., Rosi, G., and Norton, S.J. (1995). N,S-bis-fluorenylmethoxycarbonylglutathione: a new, very potent inhibitor of mammalian glyoxalase II. Biochem. Mol. Biol. Int. *35*, 763–771.

Guha, M.K., Vander Jagt, D.L., and Creighton, D.J. (1988). Diffusion-dependent rates for the hydrolysis reaction catalyzed by glyoxalase II from rat erythrocytes. Biochemistry *27*, 8818–8822.

Hamilton, D.S. and Creighton, D.J. (1992). Inhibition of glyoxalase I by the enediol mimic S-(N-hydroxy-N-methylcarbamoyl)glutathione. The possible basis of a tumor-selective anticancer strategy. J. Biol. Chem. *267*, 24933–24936.

Iozef, R., Rahlfs, S., Chang, T., Schirmer, H., and Becker, K. (2003). Glyoxalase I of the malarial parasite *Plasmodium falciparum*: evidence for subunit fusion. FEBS Lett. *554*, 284–288.

Irsch, T. and Krauth-Siegel, R.L. (2004). Glyoxalase II of African trypanosomes is trypanothione-dependent. J. Biol. Chem. *279*, 22209–22217.

Kawatani, M., Okumura, H., Honda, K., Kanoh, N., Muroi, M., Dohmae, N., Takami, M., Kitagawa, M., Futamura, Y., Imoto, M., et al. (2008). The identification of an osteoclastogenesis inhibitor through the inhibition of glyoxalase I. Proc. Natl. Acad. Sci. USA *105*, 11691–11696.

Laemmli, U.K. (1970). Cleavage of structural proteins during the assembly of the head of bacteriophage T4. Nature *227*, 680–685.

Marasinghe, G.P., Sander, I.M., Bennett, B., Periyannan, G., Yang, K.W., Makaroff, C.A., and Crowder, M.W. (2005). Structural studies on a mitochondrial glyoxalase II. J. Biol. Chem. *280*, 40668–40675.

McKay, G.A. and Wright, G.D. (1995). Kinetic mechanism of aminoglycoside phosphotransferase type IIIa. Evidence for a Theorell-Chance mechanism. J. Biol. Chem. *270*, 24686–24692.

Miller, A.G., Smith, D.G., Bhat, M., and Nagaraj, R.H. (2006). Glyoxalase I is critical for human retinal capillary pericyte survival under hyperglycemic conditions. J. Biol. Chem. *281*, 11864–11871.

Mitic, N., Smith, S.J., Neves, A., Guddat, L.W., Gahan, L.R., and Schenk, G. (2006). The catalytic mechanisms of binuclear metallohydrolases. Chem. Rev. *106*, 3338–3363.

Nagaraj, R.H., Shipanova, I.N., and Faust, F.M. (1996). Protein cross-linking by the Maillard reaction. Isolation, characterization, and *in vivo* detection of a lysine-lysine cross-link derived from methylglyoxal. J. Biol. Chem. *271*, 19338–19345.

Oya, T., Hattori, N., Mizuno, Y., Miyata, S., Maeda, S., Osawa, T., and Uchida, K. (1999). Methylglyoxal modification of protein. Chemical and immunochemical characterization of methylglyoxal-arginine adducts. J. Biol. Chem. *274*, 18492–18502.

O'Young, J., Sukdeo, N., and Honek, J.F. (2007). *Escherichia coli* glyoxalase II is a binuclear zinc-dependent metalloenzyme. Arch. Biochem. Biophys. *459*, 20–26.

Padmanabhan, P.K., Mukherjee, A., and Madhubala, R. (2006). Characterization of the gene encoding glyoxalase II from *Leishmania donovani*: a potential target for anti-parasite drugs. Biochem. J. *393*, 227–234.

Penninckx, M.J., Jaspers, C.J., and Legrain, M.J. (1983). The glutathione-dependent glyoxalase pathway in the yeast *Saccharomyces cerevisiae*. J. Biol. Chem. *258*, 6030–6036.

Ridderström, M. and Mannervik, B. (1997). Molecular cloning and characterization of the thiolesterase glyoxalase II from *Arabidopsis thaliana*. Biochem. J. *322*, 449–454.

Ridderström, M., Saccucci, F., Hellman, U., Bergman, T., Principato, G., and Mannervik, B. (1996). Molecular cloning, heterologous expression, and characterization of human glyoxalase II. J. Biol. Chem. *271*, 319–323.

Ridderström, M., Jemth, P., Cameron, A.D., and Mannervik, B. (2000). The active-site residue tyr-175 in human glyoxalase II contributes to binding of glutathione derivatives. Biochim. Biophys. Acta *1481*, 344–348.

Rudolph, F.B. (1979). Product inhibition and abortive complex formation. Methods Enzymol. *63*, 411–436.

Schilling, O., Wenzel, N., Naylor, M., Vogel, A., Crowder, M., Makaroff, C., and Meyer-Klaucke, W. (2003). Flexible metal binding of the metallo-β-lactamase domain: glyoxalase II incorporates iron, manganese, and zinc *in vivo*. Biochemistry *42*, 11777–11786.

Segel, I.H. (1993). Enzyme Kinetics: Behavior and Analysis of Rapid Equilibrium and Steady State Enzyme Systems (New York, USA: John Wiley & Sons, Inc.) pp. 544–555, pp. 593–606.

Sousa Silva, M., Ferreira, A.E., Tomás, A.M., Cordeiro, C., and Ponces Freire, A. (2005). Quantitative assessment of the glyoxalase pathway in *Leishmania infantum* as a therapeutic target by modelling and computer simulation. FEBS J. *272*, 2388–2398.

Sousa Silva, M., Barata, L., Ferreira, A.E., Romão, S., Tomás, A.M., Ponces Freire, A., and Cordeiro, C. (2008). Catalysis and structural properties of *Leishmania infantum* glyoxalase II: trypanothione specificity and phylogeny. Biochemistry *47*, 195–204.

Thompson, J.D., Higgins, D.G., and Gibson, T.J. (1994). CLUSTAL W: improving the sensitivity of progressive multiple sequence alignment through sequence weighting, position-specific gap penalties and weight matrix choice. Nucleic Acids Res. *22*, 4673–4680.

Thornalley, P.J. (1990). The glyoxalase system: new developments towards functional characterization of a metabolic pathway fundamental to biological life. Biochem. J. *269*, 1–11.

Thornalley, P.J. (1996). Pharmacology of methylglyoxal: formation, modification of proteins and nucleic acids, and enzymatic detoxification – a role in pathogenesis and antiproliferative chemotherapy. Gen. Pharmacol. *27*, 565–573.

Tsuruo, T., Naito, M., Tomida, A., Fujita, N., Mashima, T., Sakamoto, H., and Haga, N. (2003). Molecular targeting therapy of cancer: drug resistance, apoptosis and survival signal. Cancer Sci. *94*, 15–21.

Uotila, L. (1973). Purification and characterization of S-2-hydroxyacylglutathione hydrolase (glyoxalase II) from human liver. Biochemistry *12*, 3944–3951.

Vander Jagt, D.L. (1989). The glyoxalase system. In: Glutathione, Chemical, Biochemical and Medical Aspects, D. Dolphin, R. Poulson, and O. Avramovic, eds. (New York, USA: Wiley Interscience) pp. 597–641.

Vander Jagt, D.L., Hunsaker, L.A., Campos, N.M., and Baack, B.R. (1990). D-lactate production in erythrocytes infected with *Plasmodium falciparum*. Mol. Biochem. Parasitol. *42*, 277–284.

Wendler, A., Irsch, T., Rabbani, N., Thornalley, P.J., and Krauth-Siegel, R.L. (2009). Glyoxalase II does not support methylglyoxal detoxification but serves as a general trypanothione thioesterase in African trypanosomes. Mol. Biochem. Parasitol. *163*, 19–27.

Zang, T.M., Hollman, D.A., Crawford, P.A., Crowder, M.W., and Makaroff, C.A. (2001). *Arabidopsis* glyoxalase II contains a zinc/iron binuclear metal center that is essential for substrate binding and catalysis. J. Biol. Chem. *276*, 4788–4795.

Received June 2, 2009; accepted July 16, 2009